Oxygen partial pressure dependence of surface space charge formation in donor-doped $SrTiO_3$

Michael Andrä, Filip Dvořák, Mykhailo Vorokhta, Slavomír Nemšák, Vladimír Matolín, Claus M. Schneider, Regina Dittmann, Felix Gunkel, David N. Mueller, and Rainer Waser

Citation: APL Materials **5**, 056106 (2017); doi: 10.1063/1.4983618
View online: http://dx.doi.org/10.1063/1.4983618
View Table of Contents: http://aip.scitation.org/toc/apm/5/5
Published by the American Institute of Physics

Oxygen partial pressure dependence of surface space charge formation in donor-doped $SrTiO_3$

Michael Andrä,[1,a] Filip Dvořák,[2] Mykhailo Vorokhta,[2] Slavomír Nemšák,[1] Vladimír Matolín,[2] Claus M. Schneider,[1] Regina Dittmann,[1] Felix Gunkel,[1,3] David N. Mueller,[1] and Rainer Waser[1,3]

[1]*Peter Grünberg Institut, Forschungszentrum Jülich GmbH, Jülich 52425 Germany*
[2]*Department of Surface and Plasma Science, MFF UK, Charles University, Prague 18000, Czech Republic*
[3]*Institute of Electronic Materials (IWE2), RWTH Aachen University, Aachen 52074, Germany*

(Received 8 March 2017; accepted 3 May 2017; published online 19 May 2017)

In this study, we investigated the electronic surface structure of donor-doped strontium titanate. Homoepitaxial 0.5 wt. % donor-doped $SrTiO_3$ thin films were analyzed by *in situ* near ambient pressure X-ray photoelectron spectroscopy at a temperature of 770 K and oxygen pressures up to 5 mbar. Upon exposure to an oxygen atmosphere at elevated temperatures, we observed a rigid binding energy shift of up to 0.6 eV towards lower binding energies with respect to vacuum conditions for all $SrTiO_3$ core level peaks and the valence band maximum with increasing oxygen pressure. The rigid shift is attributed to a relative shift of the Fermi energy towards the valence band concomitant with a negative charge accumulation at the surface, resulting in a compensating electron depletion layer in the near surface region. Charge trapping effects solely based on carbon contaminants are unlikely due to their irreversible desorption under the given experimental conditions. In addition, simple reoxygenation of oxygen vacancies can be ruled out as the high niobium dopant concentration dominates the electronic properties of the material. Instead, the negative surface charge may be provided by the formation of cation vacancies or the formation of charged oxygen adsorbates at the surface. Our results clearly indicate a pO_2-dependent surface space charge formation in donor-doped $SrTiO_3$ in oxidizing conditions. [http://dx.doi.org/10.1063/1.4983618]

In recent years, donor-doped strontium titanate (n-$SrTiO_3$) has gained a lot of attention as a model material for various applications, such as gas sensing[1,2] or resistive switching.[3–5] In addition, it is widely used as a quasi-metallic substrate material for oxidic water splitting catalysts,[6] superconducting thin films,[7] ferroelectric tunnel junctions,[8] or resistive switching devices.[9,10]

Bulk n-$SrTiO_3$ is mostly referred to as a degenerate n-type semiconductor. However, recent research on n-$SrTiO_3$ indicated the existence of a surface space charge layer rendering its surface properties more complex: Ohtomo *et al.* observed a surface electron depletion in La-doped $SrTiO_3$ thin films at temperatures below 300 K and related it to an intrinsic surface pinning potential of about 0.7 eV.[11] In addition, Mikheev *et al.* attributed the magnitude of the resistive switching properties of a Pt/Nb:$SrTiO_3$ junction to charges trapped in an unintentional contamination layer.[4] Wang *et al.* connected a surface band bending to anti-domain boundaries in different reconstructions of the $SrTiO_3$ (110) surface after annealing treatments in different pO_2.[12] Moreover, Marchewka *et al.* revealed the existence of an electron depletion layer in Pt/Fe:$SrTiO_3$/Nb:$SrTiO_3$ structures extending into the Nb-doped bottom electrode that can be associated with acceptor-type interface defects. They suggested the presence of strontium vacancies (V''_{Sr}) at the Fe:$SrTiO_3$/Nb:$SrTiO_3$ interface.[13] These

[a]Electronic mail: m.andrae@fz-juelich.de

findings are complemented by Meyer *et al.* who recently proposed a high temperature surface oxidation model that associates electron depletion in the near surface region of *n*-$SrTiO_3$ in oxidizing conditions with the incorporation of negatively charged surface V''_{Sr}, accompanied by the precipitation of strontium oxide (SrO) at the surface.[14–17] A comparable scenario has been proposed also for electron gases formed at interfaces of $SrTiO_3$.[18–20]

Classical defect chemistry of donor-doped bulk $SrTiO_3$ is generally accepted for elevated temperatures above 1200 K.[21] At lower temperatures, however, it might not be possible to equilibrate either of the ionic sublattices in the entire sample due to sluggish ionic movement. This would freeze out some of the concentrations, leading to an effective charge separation at the surface.[15,20] The lower temperature limit at which the surface defect chemistry of the oxygen and strontium sublattices needs to be considered is already well investigated for acceptor-doped $SrTiO_3$. However, it is much more complex for donor-doped $SrTiO_3$, due to long equilibration times, secondary phase formation,[22] and the stronger influence of cations as electronic charge compensating species.[15] Complementing defect chemical considerations, at lower temperatures, the presence of charged adsorbates might influence *n*-$SrTiO_3$ surfaces in oxidizing conditions. Setvin *et al.* showed the existence of oxygen molecules forming superoxides at TiO_2 surfaces below 300 K.[23,24] Similarly, charged oxygen adsorbate species are proposed on perovskite surfaces at comparably high temperatures, their concentration diminishing with increasing temperature though.[25] Far above room temperature, the presence of any of those oxygen species on *n*-$SrTiO_3$ surfaces is still unconfirmed and any effect on the space charge formation has not been quantified so far. Thus, up to now, it is not known, whether intrinsic electronic surface states,[11] or unintentional defect layers due to carbonate adsorbates,[4] or possibly chemisorbed charged oxygen molecules such as observed for TiO_2,[23,24,26] or intrinsic ionic surface defects, namely, V''_{Sr},[15] can cause the observed surface space charge layer effect in *n*-$SrTiO_3$[13] and its dependence on the oxygen partial pressure (pO_2).

So far, the majority of studies used simulations and *ex situ* experiments to investigate the surface properties of *n*-$SrTiO_3$. In this paper, we now study the surface electronic properties of *n*-$SrTiO_3$ directly by *in situ* near ambient pressure X-ray photoelectron spectroscopy (NAP-XPS)[27,28] on stoichiometric 0.5 wt. % Nb-doped $SrTiO_3$ (Nb:$SrTiO_3$) thin films at a temperature of 770 K and different pO_2. NAP-XPS provides a unique tool for the *in situ* study of electronic and chemical processes in different gas atmospheres up to a pressure of several millibars.[27] For this, the sample stack is placed in a closed cell, isolated from the surrounding ultra high vacuum (UHV) measurement setup (Fig. 1). Due to the reduced mean free path of emitted photoelectrons at high pressures inside the sample space, a differentially pumped detector nozzle is placed close to the sample surface (0.3 mm) and kept at an absolute pressure below 10^{-8} mbar. These measurements allow a direct access to the surface electronic structure of the *n*-$SrTiO_3$ samples as a function of pO_2 while simultaneously providing

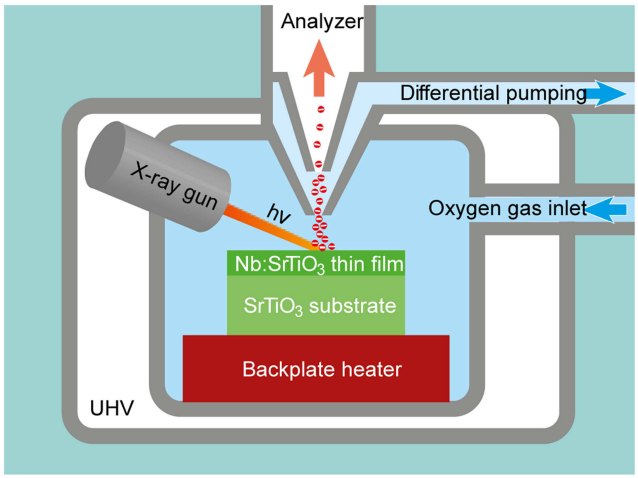

FIG. 1. Schematic illustration of the sample stack as well as the near ambient pressure X-ray photoelectron spectroscopy measurement setup.

information on the surface coverage of adsorbates and contaminants as well as on the chemical composition.

We deposited 32 nm of stoichiometric 0.5 wt. % Nb:$SrTiO_3$ by pulsed laser deposition (PLD) on a single crystalline $SrTiO_3$ (100) substrate (*CrysTec GmbH, Berlin, Germany*), using a KrF excimer laser ($\lambda = 248$ nm) with a laser energy of 50 mJ at a repetition rate of 5 Hz, a spot size of 2 mm^2, and a target-to-substrate distance of 44 mm. The film was grown in an oxygen atmosphere of 0.1 mbar at a substrate temperature of 1073 K. After the growth, the sample was quenched down to room temperature and no further treatment was performed prior to the NAP-XPS measurements. The growth process was monitored by reflection high energy electron diffraction (RHEED). Clear RHEED oscillations indicate a layer-by-layer growth of the thin film (S1 of the supplementary material). The stoichiometric growth process of the thin film was optimized by a variation of the laser fluence[29,30] and confirmed by angular dependent X-ray photoelectron spectroscopy in UHV conditions.[31,32] Further sample characterization including surface topography and X-ray diffraction data are provided in the supplementary material S1 and S2. In addition, the quality of the thin films was further confirmed by room temperature Hall measurements on 200 nm thick films verifying the carrier concentration (1.5×10^{20} cm^{-3}) and the electron mobility (6.1 cm^2/Vs) to match the expected values. Additional measurements of the low temperature mobility are shown in the supplementary material (S3). We find metallic behaviour and an electron mobility of 200 cm^2/Vs at 10 K which is in good agreement with literature values obtained at similar dopant concentrations.[21,33–35]

For a pO_2-dependent spectroscopic analysis, the thin film was investigated using a Specs^{TM} near-ambient pressure XPS instrument using an Al Kα source (1486.6 eV) and an emission angle of 90°. In all measurements, the as prepared sample was contacted from the top using a Ti strip, providing an electrical contact between the *n*-type thin film and analyzer. All constituents' core levels as well as the valence band and the carbon core level spectra were measured *in situ* at a temperature of 770 K and under different pO_2 ranging from UHV conditions (base pressure ~10^{-8} mbar) up to 5 mbar. The lowest accurately adjustable pO_2 in this measurement setup was 0.05 mbar.

Figure 2 shows the pO_2-dependent core level spectra[36] of oxygen 1s and carbon 1s (a), titanium 2p (b), and strontium 3d (c), as well as the valence band region (d) obtained at room temperature (dashed spectra) and at an elevated temperature of 770 K (solid spectra). Initial spectra were taken at room temperature and UHV (dashed top spectra) on as-prepared samples. As can be seen from the O1s and the C1s spectra (Fig. 2(a)), a significant amount of carbon adsorbates and contaminants is present at the thin film surface resulting from exposure to air after the PLD growth process and *ex situ* transfer into the NAP-XPS setup. Upon heating to 770 K in UHV, a reduction of the carbon adsorbates and contaminants is clearly visible in the O1s and the C1s spectra. Subsequently, the pO_2 was increased stepwise from 0.05 mbar to 5 mbar while a temperature of 770 K was maintained. All carbon adsorbates and contaminants are removed from the surface upon heating at a pO_2 above 0.05 mbar. Furthermore, no traces of other typical surface contaminants (S, Si) were detected.

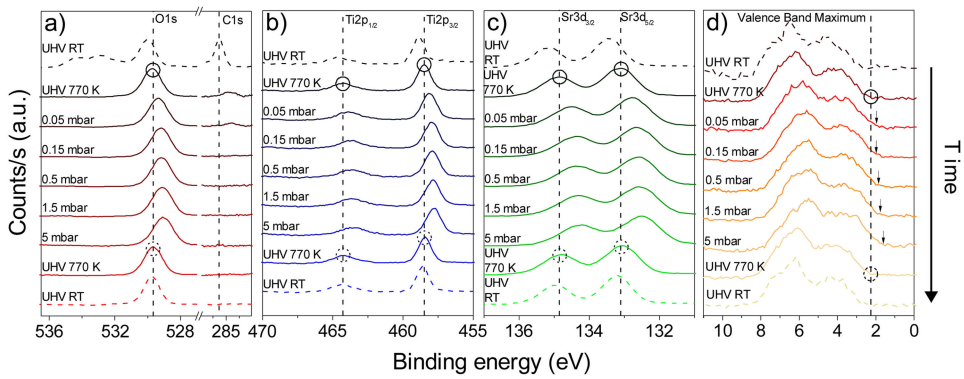

FIG. 2. Core level spectra of O1s and C1s (a), Ti2p (b), and Sr3d (c), as well as the valence band region (d) of a 32 nm thick Nb:$SrTiO_3$ film at room temperature (dashed spectra) and 770 K (solid spectra). The dashed vertical lines indicate the position of the characteristic binding energies at the first measurement at 770 K and in UHV conditions (solid circles). The dashed circles indicate the characteristic binding energies at the second measurement at 770 K and in UHV conditions.

With increasing pO_2, a significant shift towards lower binding energies (BEs) is detected for all the characteristic core level spectra and the valence band maximum (VBM). To emphasize the BE shifts, the vertical dashed lines indicate the characteristic binding energy of O1s, Ti2p, Sr3d, and the VBM at the initial measurement at UHV conditions at 770 K (solid circles). Full reversibility of the BE shifts was confirmed by a following set of spectra taken again in UHV conditions at 770 K (dashed circles), pointing towards a reversible underlying surface process, solely governed by the ambient pO_2.

Finally, the thin film was cooled down to room temperature while the UHV conditions were maintained (dashed bottom spectra). As can be seen from the lack of spectral intensities in the C1s core level spectra, the surface was cleaned permanently at an increased temperature. Furthermore, the core level spectra measured at room temperature in UHV conditions show that upon cooling the characteristic BE shifts just slightly towards higher values as compared to the ones that had been measured in the first measurement at room temperature and UHV conditions. The shift between the top and bottom dashed spectra, respectively, at room temperature and in UHV conditions might be due to the absence of carbon adsorbates and contaminants in the second measurement. Hence, there is an apparent effect of carbon-type surface adsorbates on the electronic surface configuration. However, due to reversibility of the BE shift in UHV conditions without the reappearance of the C1 s peak, the pO_2-dependent shifts observed at 770 K cannot be explained by surface carbon contaminants solely. It should be noted that X-ray beam-related charging of the sample typically results in a shift of the apparent BE towards higher values.[37] Considering that intuitively $SrTiO_3$ should be more conducting in UHV than in oxidizing atmospheres, our sample shows the opposite behaviour, making charging effects on the apparent BE unlikely. To more rigorously exclude charging, we performed additional reference measurements on an Au electrode deposited on the sample with an additional Ti interlayer to ensure an ohmic contact to the thin film. As shown in the supplementary material S4, no shift with pO_2 is evident for the Au4f spectra.

In order to investigate the observed shift in more detail, the BE values of all core levels were fitted by *KolXPD* software using a Shirley background subtraction and an appropriate combination of Voigt peaks and doublets. We fitted two Voigt functions for the O1s peak, reflecting unsaturated surface lattice oxygen and saturated lattice oxygen with the similar BE shift,[38] one Voigt function for the C1s peak, two separate Voigt functions with different FWHM[39] and a fixed distance for the Ti2p peaks, one Voigt doublet with fixed peak separations and area ratios corresponding to the spin orbit splitting for the Sr3d peaks. To determine the VBM, the intersection of a linear approximation of the leading edge of the VB spectra and background was determined (indicated by vertical arrows in Fig. 2(d)).[40] While increasing/deceasing pO_2, none of the Ti core level spectra shows any sign of a Ti^{3+} component, indicating a Ti^{3+} concentration below the detection limit and a negligible contribution of oxygen vacancies for the thin film's electronic properties even in UHV conditions. With varying pO_2, the core level spectra generally show slight broadening, similarly observed in all core levels (see Fig. S6 in the supplementary material). The Sr core level spectra additionally show an increasingly shallower intensity valley between the $3d_{3/2}$ and $3d_{5/2}$ peaks. These changes in spectral shape may directly result from a changed potential profile in the surface space charge layer.[41,42] Similar intensity changes in the Sr core level, however, have also been assigned to SrO[17,43] or hydroxide ($Sr(OH)_2$)[41] surface phase formation. Neither the spectral differences in the O1s,[44] the Sr3d,[17,45] in the Ti2p[46] nor any spectral changes in the VB spectra[47] allow for an unambiguous interpretation as chemical changes. In fact, both scenarios (band bending and/or chemical changes) can describe the changes in the peak shapes equally well (cf., S6 in the supplementary material). It should be noted though that the signal to noise ratio is highly dependent on the absolute pressure in the measurement chamber, which will increase the detection limit for determining chemical changes at higher pO_2.

Figure 3 shows the BE values of the core levels (a), the difference between the Fermi energy (E_F), referenced by a gold standard measurement, and the valence band maximum as well as the estimated temperature dependent position of the conduction band minimum (CBM)[21] (b), and the relative BE shift of the different core level spectra and the VBM with respect to the initial UHV measurements (c) at 770 K. As discussed above, all characteristic BE shifts towards lower values while increasing the pO_2. The measured position of the difference between E_F and the VBM at an absolute pressure of 10^{-8} mbar is close to the temperature dependent CBM expected at 770 K (Fig. 3(b), dashed line),[21]

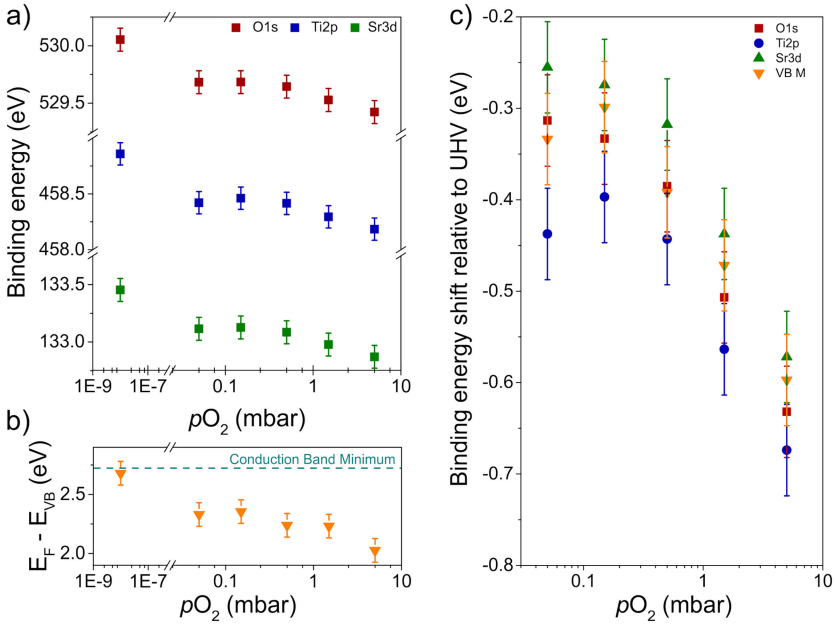

FIG. 3. Position of the characteristic BE of $SrTiO_3$ core levels (a), the energy difference between the Fermi energy and the valence band maximum as well as the temperature dependent conduction band minimum (b). BE shift relative to measurements in UHV conditions (c). For a better comparability, the x-axis in Fig. 3(a) is interrupted from 3×10^{-7} mbar to 3×10^{-2} mbar.

indicating that the Fermi energy of the thin film is close to the conduction band.[48] As expected from classical semiconductors, this is consistent with a full ionization of shallow donor dopants and the reported small ionization energy of niobium dopants in $SrTiO_3$ of 0.08 eV.[49]

The more the pO_2 is increased, the more the VBM is shifted towards lower BE, indicating a continuous shift of the Fermi energy deeper into the band gap. Fig. 3(c) summarizes the shift of the BE relative to the measured value at an absolute pressure of 10^{-8} mbar. It is clearly visible that all core level spectra and the VBM shift with an increasing pO_2. The relative shifts of the different core levels nearly overlap on a single line with the one of the VBM, indicating that all peaks shift rigidly with pO_2 within the experimental uncertainty. In the rigid band model, the apparent BE of the core levels is governed solely by the Fermi energy of the sample, it is therefore a direct measure of the concentration of electrons.[48,50,51] Consequently, the measured rigid shift of all core level spectra of $SrTiO_3$ and the VBM can be explained by a mere shift of the Fermi energy at the surface, i.e., an effective change of the conduction band filling.

The maximum shift at 770 K and a pO_2 of 5 mbar for the different measured BE values is about 0.6 eV, which is the same order of magnitude as the surface pinning potential observed in Ref. 11

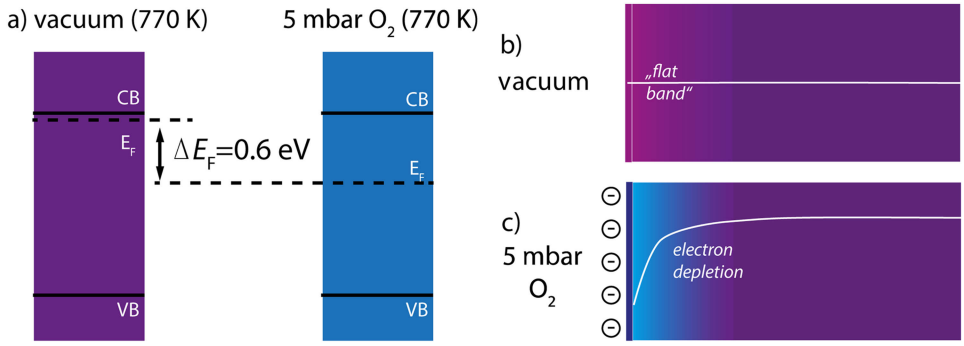

FIG. 4. Schematic illustration of the relative positions of the Fermi energy in UHV conditions and 5 mbar pO_2 at 770 K (a). The surface carrier concentration in the electronic compensation (b) and in the ionic compensation regime (c) resulting in a flat band and electron depletion, respectively.

and the reported surface potential obtained from a defect chemical oxidation model at 1500 K.[15] Furthermore, Higuchi *et al.* found the differences in the BE of 0.7 eV for 2 at. % donor-doped and 2 at. % acceptor-doped $SrTiO_3$ due to a similar lowering of the Fermi energy in acceptor-doped $SrTiO_3$.[51] In fact, this suggests that the surface of *n*-$SrTiO_3$ rather acts like acceptor-doped or undoped $SrTiO_3$ under oxidizing conditions, implying a significant pO_2-dependent change in the electronic surface properties.

Figure 4 illustrates the relative positions of the Fermi energy in UHV conditions and 5 mbar pO_2 at 770 K (a) as indicated by the NAP-XPS results. In UHV, the position of the Fermi energy close to the conduction band suggests a bulk-like behavior of the *n*-$SrTiO_3$ surface, with a constant carrier concentration over the entire thickness of the thin film (flat band). In contrast, at increased pO_2, the observed relative shift of the Fermi energy into the band gap indicates a reduction of the electron concentration in the *n*-$SrTiO_3$ thin film, implying a negative surface charge that is reversibly controlled by varying the ambient oxygen atmosphere (Fig. 4(c)).

Using an Al-Kα X-ray source, the inelastic mean free path of the XPS measurement setup is about 1.5 nm – 2.5 nm depending on the core level,[42] by definition making 63% of the signals originating from these depths. Thus, XPS is a surface sensitive technique and the observed peak shift provides information mainly on the near-surface electron concentration. Using a parabolic potential approach the potential profile and the corresponding electrostatic decay length $d_{SCR} = \sqrt{(-2\varepsilon_r\varepsilon_0\Phi)/(eN)}$ can be estimated to be about 7 nm at 5 mbar O_2. Here, we use the vacuum permittivity ε_0, the elementary charge e, and the dopant concentration N. Φ is defined by the measured BE shift, thus assuming a flat band in UHV. The relative dielectric constant $\varepsilon_r \approx 105$ has been considered temperature dependent,[52] while an electric field dependence has been neglected.[53] Hence, assuming a process limited to the surface, it can be inferred that the electron concentration deep in the thin film is given by the niobium dopant concentration. The resulting electron concentration difference between the bulk and the surface of the thin film thus implies the formation of a surface space charge layer and with that, a band bending that can be controlled in a reversible manner by varying the pO_2.

The systematic and reversible character of the surface space charge formation as well as the disappearance of any observable carbon peak intensity makes a merely contaminants-based scenario unlikely. Instead, the negative surface charge might result from different effects. For one, at elevated temperatures and different oxygen partial pressures, varying defect concentrations at the surface may provide that negative surface charge. The expected concentration of donor-type oxygen vacancies at the given temperature and oxygen partial pressure (10^{18} cm^{-3} and below)[21,34] is significantly lower than the niobium dopant concentration. Therefore, a varying oxygen vacancy concentration alone would not provide sufficient charge for a significant change of the surface space charge region in highly-doped $SrTiO_3$. Instead, charged cation vacancies – in *n*-$SrTiO_3$ most likely V''_{Sr},[15,17,21] – may be involved in space charge formation in oxidizing conditions as their concentration can become as high as the dopant concentration and even exceed it in the near-surface region.[15] However, the temperature of 770 K in our experiments would be remarkably low for the formation of Sr vacancy defects, which are typically only considered at temperatures well above 1000 K due to kinetic limitations in the bulk.[15,20,21] However, due to the localization of the predicted effect at the surface, there would be no need for an ionic movement and hence the formation of V''_{Sr} at the surface might be possible even at lower temperatures.

Besides intrinsic defects, another possible origin of the negative surface charge that has to be considered is charged adsorbates. An increasing concentration of oxygen molecules may chemisorb at the surface in oxidizing conditions leading to a charge transfer from the sample to the oxygen molecule and a Taguchi-type[26] space charge layer. Such a formation of a surface coverage with chemisorbed oxygen species is considered typically at room temperature and below.[23,24] However, the existence of charged oxygen species at elevated temperatures has been discussed on other perovskite type oxides (e.g. $(La,Sr)MnO_{3-\delta}$[25]), with finite concentrations up to 1000 K and thus might be considered on $SrTiO_3$, too.[22,54] Hence, the adsorption of charged oxygen molecules might be possible even at higher temperatures. From the observed shift of the Fermi energy, it is possible to determine the maximum negative surface charge to $\sim 10^{14}$ e/cm^2 which corresponds to a possible surface coverage of ~8% and ~16% for V''_{Sr} and chemisorbed charged oxygen molecules, respectively. Keeping the inelastic mean free path of approximately 2.5 nm for the kinetic energies of the electrons observed here in mind, the

relative signal of the charged species covering the surface would be 1% or 2%, respectively, which is at the lower end of the detection limit.

Even though further investigations are desirable to unambiguously clarify the origin of the negative surface charge, the observed formation of a pO_2-dependent surface space charge layer in n-$SrTiO_3$ already suggests a complexity beyond purely carbon contamination-based effects or intrinsic surface states established at moderate temperatures. The observed complexity of the space charge layer may furthermore allow for the pO_2-control of the electronic properties of n-$SrTiO_3$ also beyond the classical bulk high temperature defect chemistry.

In conclusion, we have shown that n-$SrTiO_3$ forms a pO_2-dependent surface space charge layer in which electrons are depleted. With an increasing pO_2, the relative position of the Fermi energy at the surface shifts continuously from the conduction band edge deeper into the band gap. At a maximum pO_2 of 5 mbar, the Fermi energy is measured about 0.6 eV below the conduction band edge. This shift reflects a pO_2-dependent negative surface charge, resulting in space charge formation and consequently band bending. Oxygen vacancies are unlikely to be the origin of the surface charge, since the electronic properties of the thin film are dominated by the donor dopant concentration. In addition, we did not observe any carbon related contaminants at high temperatures and comparably low pO_2. Therefore, effects solely based on charged carbon contaminants at the surface are unlikely under experimental conditions, too. Instead, a negative surface charge may be caused by the formation of cation vacancies, namely, V''_{Sr}, or the formation of charged oxygen adsorbates at the surface. The experimental findings are of key importance for the research not only on niobium-doped $SrTiO_3$ itself but also on any oxide thin films grown on Nb:$SrTiO_3$ substrates at elevated temperature and high pO_2, as the conductivity of the substrate – one of the main arguments for its choice – might be strongly influenced depending on the actual pO_2.

See supplementary material for more detailed information on the stoichiometric thin film growth (S1-S3), gold (Au4f) reference XPS measurements (S4), a detailed discussion of Ti^{3+} contributions (S5) and pO_2-dependent changes in the Sr3d and Ti2p core level spectra (S6).

The authors acknowledge the CERIC-ERIC Consortium for the access to experimental facilities and financial support. R.D. thanks the W2/W3-program of the Helmholtz association. The authors want to thank K. Skaja and C. Baeumer for scientific discussions about the XPS spectra.

[1] A. M. Schultz, T. D. Brown, and P. R. Ohodnicki, J. Phys. Chem. C **119**, 6211 (2015).
[2] R. Meyer and R. Waser, Sens. Actuators, B **101**, 335 (2004).
[3] C. Baeumer, N. Raab, T. Menke, C. Schmitz, R. Rosezin, P. M. Müller, M. Andrä, V. Feyer, R. Bruchhaus, F. Gunkel, C. M. Schneider, R. Waser, and R. Dittmann, Nanoscale **8**, 13967 (2016).
[4] E. Mikheev, J. Hwang, A. P. Kajdos, A. J. Hauser, and S. Stemmer, Sci. Rep. **5**, 11079 (2015).
[5] C. Rodenbücher, T. Gensch, W. Speier, U. Breuer, M. Pilch, H. Hardtdegen, M. Mikulics, E. Zych, R. Waser, and K. Szot, Appl. Phys. Lett. **103**, 162904 (2013).
[6] K. J. May, D. P. Fenning, T. Ming, W. T. Hong, D. Lee, K. A. Stoerzinger, M. D. Biegalski, A. M. Kolpak, and Y. Shao-Horn, J. Phys. Chem. Lett. **6**, 977 (2015).
[7] J. Ge, Z. Liu, C. Liu, C. Gao, D. Qian, Q. Xue, Y. Liu, and J. Jia, Nat. Mater. **14**, 285 (2015).
[8] Z. Wen, Di Wu, and A. Li, Appl. Phys. Lett. **105**, 052910 (2014).
[9] R. Waser, R. Dittmann, G. Staikov, and K. Szot, Adv. Mater. **21**, 2632 (2009).
[10] R. Muenstermann, T. Menke, R. Dittmann, and R. Waser, Adv. Mater. **22**, 4819 (2010).
[11] A. Ohtomo and H. Y. Hwang, Appl. Phys. Lett. **84**, 1716 (2004).
[12] Z. Wang, X. Hao, S. Gerhold, M. Schmid, C. Franchini, and U. Diebold, Phys. Rev. B **90**, 035436 (2014).
[13] A. Marchewka, D. Cooper, C. Lenser, S. Menzel, H. Du, R. Dittmann, R. E. Dunin-Borkowski, and R. Waser, Sci. Rep. **4**, 6975 (2014).
[14] R. Meyer, R. Waser, J. Helmbold, and G. Borchardt, Phys. Rev. Lett. **90**, 105901 (2003).
[15] R. Meyer, A. F. Zurhelle, R. A. De Souza, R. Waser, and F. Gunkel, Phys. Rev. B **94**, 115408 (2016).
[16] H. Wei, L. Beuermann, J. Helmbold, G. Borchardt, V. Kempter, G. Lilienkamp, and W. Maus-Friedrichs, J. Eur. Ceram. Soc. **21**, 1677 (2001).
[17] K. Szot, W. Speier, U. Breuer, R. Meyer, J. Szade, and R. Waser, Surf. Sci. **460**, 112 (2000).
[18] F. Gunkel, P. Brinks, S. Hoffmann-Eifert, R. Dittmann, M. Huijben, J. E. Kleibeuker, G. Koster, G. Rijnders, and R. Waser, Appl. Phys. Lett. **100**, 52103 (2012).
[19] F. Gunkel, S. Hoffmann-Eifert, R. A. Heinen, Y. Chen, N. Pryds, R. Waser, and R. Dittmann, ACS Appl. Mater. Interfaces **9**, 1086 (2017).
[20] F. Gunkel, R. Waser, A. H. H. Ramadan, R. A. De Souza, S. Hoffmann-Eifert, and R. Dittmann, Phys. Rev. B **93**, 245431 (2016).
[21] R. Moos and K. H. Härdtl, J. Am. Ceram. Soc. **80**, 2549 (1997).
[22] R. Merkle and J. Maier, Angew. Chem., Int. Ed. **47**, 3874 (2008).

[23] M. Setvin, B. Daniel, V. Mansfeldova, L. Kavan, P. Scheiber, M. Fidler, M. Schmid, and U. Diebold, Surf. Sci. **626**, 61 (2014).
[24] M. Setvin, U. Aschauer, P. Scheiber, Y. Li, W. Hou, M. Schmid, A. Selloni, and U. Diebold, Science **341**, 988 (2013).
[25] Y. A. Mastrikov, R. Merkle, E. Heifets, E. A. Kotomin, and J. Maier, J. Phys. Chem. C **114**, 3017 (2010).
[26] T. Seiyama, A. Kato, K. Fujiishi, and M. Nagatani, Anal. Chem. **34**, 1502 (1962).
[27] D. F. Ogletree, H. Bluhm, G. Lebedev, C. S. Fadley, Z. Hussain, and M. Salmeron, Rev. Sci. Instrum. **73**, 3872 (2002).
[28] S. Yamamoto, H. Bluhm, K. Andersson, G. Ketteler, H. Ogasawara, M. Salmeron, and A. Nilsson, J. Phys.: Condens. Matter **20**, 184025 (2008).
[29] D. J. Keeble, S. Wicklein, L. Jin, C. L. Jia, W. Egger, and R. Dittmann, Phys. Rev. B **87**, 195409 (2013).
[30] F. Gunkel, S. Wicklein, P. Brinks, S. Hoffmann-Eifert, M. Huijben, G. Rijnders, R. Waser, and R. Dittmann, Nanoscale **7**, 1013 (2015).
[31] S. Wicklein, A. Sambri, S. Amoruso, X. Wang, R. Bruzzese, A. Koehl, and R. Dittmann, Appl. Phys. Lett. **101**, 131601 (2012).
[32] C. Baeumer, C. Xu, F. Gunkel, N. Raab, R. A. Heinen, A. Koehl, and R. Dittmann, Sci. Rep. **5**, 11829 (2015).
[33] A. Verma, A. P. Kajdos, T. A. Cain, S. Stemmer, and D. Jena, Phys. Rev. Lett. **112**, 216601 (2014).
[34] A. Spinelli, M. A. Torija, C. Liu, C. Jan, and C. Leighton, Phys. Rev. B **81**, 155110 (2010).
[35] Y. Kozuka, Y. Hikita, C. Bell, and H. Y. Hwang, Appl. Phys. Lett. **97**, 12107 (2010).
[36] R. T. Haasch, E. Breckenfeld, and L. W. Martin, Surf. Sci. Spectra **21**, 87 (2014).
[37] A. Cros, J. Electron Spectrosc. Relat. Phenom. **59**, 1 (1992).
[38] K. A. Stoerzinger, W. T. Hong, E. J. Crumlin, H. Bluhm, M. D. Biegalski, and Y. Shao-Horn, J. Phys. Chem. C **118**, 19733 (2014).
[39] M. Oku, H. Matsuta, K. Wagatsuma, Y. Waseda, and S. Kohiki, J. Electron Spectrosc. Relat. Phenom. **105**, 211 (1999).
[40] S. A. Chambers, T. Droubay, T. C. Kaspar, and M. Gutowski, J. Vac. Sci. Technol. B **22**, 2205 (2004).
[41] S. A. Chambers, Y. Du, R. B. Comes, S. R. Spurgeon, and P. V. Sushko, Appl. Phys. Lett. **110**, 082104 (2017).
[42] M. F. Lichterman, M. H. Richter, B. S. Brunschwig, N. S. Lewis, and H. Lewerenz, "Operando X-ray photoelectron spectroscopic investigations of the electrochemical double layer at Ir/KOH(aq) interfaces," J. Electron Spectrosc. Relat. Phenom. (to be published).
[43] C. Baeumer, C. Schmitz, A. H. H. Ramadan, H. Du, K. Skaja, V. Feyer, P. Muller, B. Arndt, C. Jia, J. Mayer, R. A. De Souza, C. Michael Schneider, R. Waser, and R. Dittmann, Nat. Commun. **6**, 8610 (2015).
[44] J. W. Rogers, N. D. Shinn, J. E. Schirber, E. L. Venturini, D. S. Ginley, and B. Morosin, Phys. Rev. B **38**, 5021 (1988).
[45] T. Ohsawa, R. Shimizu, K. Iwaya, S. Shiraki, and T. Hitosugi, Appl. Phys. Lett. **108**, 161603 (2016).
[46] C. Xu, C. Baeumer, R. A. Heinen, S. Hoffmann-Eifert, F. Gunkel, and R. Dittmann, Sci. Rep. **6**, 1 (2016).
[47] L. Dudy, M. Sing, P. Scheiderer, J. D. Denlinger, P. Schuetz, J. Gabel, M. Buchwald, C. Schlueter, T. Lee, and R. Claessen, Adv. Mater. **28**, 7443 (2016).
[48] E. A. Kraut, R. W. Grant, J. R. Waldrop, and S. P. Kowalczyk, Phys. Rev. Lett. **44**, 1620 (1980).
[49] R. I. Eglitis and E. A. Kotomin, Physica B **405**, 3164 (2010).
[50] A. Nenning, A. K. Opitz, C. Rameshan, R. Rameshan, R. Blume, M. Hävecker, A. Knop-Gericke, G. Rupprechter, B. Klötzer, and J. Fleig, J. Phys. Chem. C **120**, 1461 (2016).
[51] T. Higuchi, T. Tsukamoto, N. Sata, M. Ishigame, Y. Tezuka, and S. Shin, Phys. Rev. B **57**, 6978 (1998).
[52] *Landolt-Börnstein, Zahlenwerte und Funktionen aus Naturwissenschaft und Technik, Gruppe I3: Kristall- und Festkörper, Band 16 Ferroelektrika und verwandte Substanzen, Teilband a,* edited by K.-H. Hellwege and A. M. Hellwege (Springer-Verlag, Berlin, Heidelberg, New York, 1981).
[53] R. C. Neville, B. Hoeneisen, and C. A. Mead, J. Appl. Phys. **43**, 2124 (1972).
[54] R. Merkle and J. Maier, Phys. Chem. Chem. Phys. **4**, 4140 (2002).